

66. Quark Masses

Updated March 2018 by A.V. Manohar (UC, San Diego), C.T. Sachrajda (University of Southampton), and R.M. Barnett (LBNL).

66.1. Introduction

This note discusses some of the theoretical issues relevant for the determination of quark masses, which are fundamental parameters of the Standard Model of particle physics. Unlike the leptons, quarks are confined inside hadrons and are not observed as physical particles. Quark masses therefore cannot be measured directly, but must be determined indirectly through their influence on hadronic properties. Although one often speaks loosely of quark masses as one would of the mass of the electron or muon, any quantitative statement about the value of a quark mass must make careful reference to the particular theoretical framework that is used to define it. It is important to keep this *scheme dependence* in mind when using the quark mass values tabulated in the data listings.

Historically, the first determinations of quark masses were performed using quark models. The resulting masses only make sense in the limited context of a particular quark model, and cannot be related to the quark mass parameters of the Standard Model. In order to discuss quark masses at a fundamental level, definitions based on quantum field theory must be used, and the purpose of this note is to discuss these definitions and the corresponding determinations of the values of the masses.

66.2. Mass parameters and the QCD Lagrangian

The QCD [1] Lagrangian for N_F quark flavors is

$$\mathcal{L} = \sum_{k=1}^{N_F} \bar{q}_k (i\mathcal{D} - m_k) q_k - \frac{1}{4} G_{\mu\nu} G^{\mu\nu} , \quad (66.1)$$

where $\mathcal{D} = (\partial_\mu - igA_\mu) \gamma^\mu$ is the gauge covariant derivative, A_μ is the gluon field, $G_{\mu\nu}$ is the gluon field strength, m_k is the mass parameter of the k^{th} quark, and q_k is the quark Dirac field. After renormalization, the QCD Lagrangian Eq. (66.1) gives finite values for physical quantities, such as scattering amplitudes. Renormalization is a procedure that invokes a subtraction scheme to render the amplitudes finite, and requires the introduction of a dimensionful scale parameter μ . The mass parameters in the QCD Lagrangian Eq. (66.1) depend on the renormalization scheme used to define the theory, and also on the scale parameter μ . The most commonly used renormalization scheme for QCD perturbation theory is the $\overline{\text{MS}}$ scheme.

The QCD Lagrangian has a chiral symmetry in the limit that the quark masses vanish. This symmetry is spontaneously broken by dynamical chiral symmetry breaking, and explicitly broken by the quark masses. The nonperturbative scale of dynamical chiral symmetry breaking, Λ_χ , is around 1 GeV [2]. It is conventional to call quarks heavy if $m > \Lambda_\chi$, so that explicit chiral symmetry breaking dominates (c , b , and t quarks are heavy), and light if $m < \Lambda_\chi$, so that spontaneous chiral symmetry breaking dominates (the u and d are light and s quarks are considered to be light when using $\text{SU}(3)_L \times \text{SU}(3)_R$ chiral perturbation theory). The determination of light- and heavy-quark masses is considered separately in Sec. 66.4 and Sec. 66.5 below.

2 66. Quark masses

At high energies or short distances, nonperturbative effects, such as chiral symmetry breaking, become small and one can, in principle, determine quark masses by analyzing mass-dependent effects using QCD perturbation theory. Such computations are conventionally performed using the $\overline{\text{MS}}$ scheme at a scale $\mu \gg \Lambda_\chi$, and give the $\overline{\text{MS}}$ “running” mass $\overline{m}(\mu)$. We use the $\overline{\text{MS}}$ scheme when reporting quark masses; one can readily convert these values into other schemes using perturbation theory.

The μ dependence of $\overline{m}(\mu)$ at short distances can be calculated using the renormalization group equation,

$$\mu^2 \frac{d\overline{m}(\mu)}{d\mu^2} = -\gamma(\overline{\alpha}_s(\mu)) \overline{m}(\mu), \quad (66.2)$$

where γ is the anomalous dimension which is now known to four-loop order in perturbation theory [3,4]. $\overline{\alpha}_s$ is the coupling constant in the $\overline{\text{MS}}$ scheme. Defining the expansion coefficients γ_r by

$$\gamma(\overline{\alpha}_s) \equiv \sum_{r=1}^{\infty} \gamma_r \left(\frac{\overline{\alpha}_s}{4\pi} \right)^r,$$

the first four coefficients are given by

$$\begin{aligned} \gamma_1 &= 4, \\ \gamma_2 &= \frac{202}{3} - \frac{20N_L}{9}, \\ \gamma_3 &= 1249 + \left(-\frac{2216}{27} - \frac{160}{3}\zeta(3) \right) N_L - \frac{140}{81} N_L^2, \\ \gamma_4 &= \frac{4603055}{162} + \frac{135680}{27}\zeta(3) - 8800\zeta(5) \\ &\quad + \left(-\frac{91723}{27} - \frac{34192}{9}\zeta(3) + 880\zeta(4) + \frac{18400}{9}\zeta(5) \right) N_L \\ &\quad + \left(\frac{5242}{243} + \frac{800}{9}\zeta(3) - \frac{160}{3}\zeta(4) \right) N_L^2 \\ &\quad + \left(-\frac{332}{243} + \frac{64}{27}\zeta(3) \right) N_L^3, \end{aligned}$$

where N_L is the number of active light quark flavors at the scale μ , i.e. flavors with masses $< \mu$, and ζ is the Riemann zeta function ($\zeta(3) \simeq 1.2020569$, $\zeta(4) \simeq 1.0823232$, and $\zeta(5) \simeq 1.0369278$). In addition, as the renormalization scale crosses quark mass thresholds one needs to match the scale dependence of \overline{m} below and above the threshold. There are finite threshold corrections; the necessary formulae can be found in Ref. [5].

The quark masses for light quarks discussed so far are often referred to as current quark masses. Nonrelativistic quark models use constituent quark masses, which are of order 350 MeV for the u and d quarks. Constituent quark masses model the effects of dynamical chiral symmetry breaking, and are not directly related to the quark mass parameters m_k of the QCD Lagrangian Eq. (66.1). Constituent masses are only defined in the context of a particular hadronic model.

66.3. Lattice Gauge Theory

The use of the lattice simulations for *ab initio* determinations of the fundamental parameters of QCD, including the coupling constant and quark masses (except for the top-quark mass) is a very active area of research (see the review on Lattice Quantum Chromodynamics in this *Review*). Here we only briefly recall those features which are required for the determination of quark masses. In order to determine the lattice spacing (a , i.e. the distance between neighboring points of the lattice) and quark masses, one computes a convenient and appropriate set of physical quantities (frequently chosen to be a set of hadronic masses) for a variety of input values of the quark masses. The true (physical) values of the quark masses are those which correctly reproduce the set of physical quantities being used for the calibration.

The values of the quark masses obtained directly in lattice simulations are bare quark masses, corresponding to a particular discretization of QCD and with the lattice spacing as the ultraviolet cut-off. In order for these results to be useful in phenomenological applications, it is necessary to relate them to renormalized masses defined in some standard renormalization scheme such as $\overline{\text{MS}}$. Provided that both the ultraviolet cut-off a^{-1} and the renormalization scale μ are much greater than Λ_{QCD} , the bare and renormalized masses can be related in perturbation theory. However, in order to avoid uncertainties due to the unknown higher-order coefficients in lattice perturbation theory, most results obtained recently use *non-perturbative renormalization* to relate the bare masses to those defined in renormalization schemes which can be simulated directly in lattice QCD (e.g. those obtained from quark and gluon Green functions at specified momenta in the Landau gauge [62] or those defined using finite-volume techniques and the Schrödinger functional [63]). The conversion to the $\overline{\text{MS}}$ scheme (which cannot be simulated) is then performed using continuum perturbation theory.

The determination of quark masses using lattice simulations is well established and the current emphasis is on the reduction and control of the systematic uncertainties. With improved algorithms and access to more powerful computing resources, the precision of the results has improved immensely in recent years. Vacuum polarisation effects are included with $N_f = 2$, $2 + 1$ or $N_f = 2 + 1 + 1$ flavors of sea quarks. The number 2 here indicates that the up and down quarks are degenerate. In earlier *reviews*, results were presented from simulations in which vacuum polarization effects were completely neglected (this is the so-called *quenched* approximation), leading to systematic uncertainties which could not be estimated reliably. It is no longer necessary to include quenched results in compilations of quark masses. Particularly pleasing is the observation that results obtained using different formulations of lattice QCD, with different systematic uncertainties, give results which are largely consistent with each

4 66. Quark masses

other. This gives us broad confidence in the estimates of the systematic errors. As the precision of the results approaches (or even exceeds in some cases) 1%, isospin breaking effects, including electromagnetic corrections need to be included and this is beginning to be done as will be discussed below. The results however, are still at an early stage and therefore, unless explicitly stated otherwise, the results presented below will neglect isospin breaking.

Members of the lattice QCD community have organised a Flavour Lattice Averaging Group (FLAG) which critically reviews quantities computed in lattice QCD relevant to flavor physics, including the determination of light quark masses, against stated quality criteria and presents its view of the current status of the results. The latest (2nd) edition reviewed lattice results published before November 30th 2013 [16].

66.4. Light quarks

In this section we review the determination of the masses of the light quarks u , d and s from lattice simulations and then discuss the consequences of the approximate chiral symmetry.

66.4.1. Lattice Gauge Theory: The most reliable determinations of the strange quark mass m_s and of the average of the up and down quark masses $m_{ud} = (m_u + m_d)/2$ are obtained from lattice simulations. As explained in section C above, the simulations are generally performed with degenerate up and down quarks ($m_u = m_d$) and so it is the average which is obtained directly from the computations. Below we discuss attempts to derive m_u and m_d separately using lattice results in combination with other techniques, but we start by briefly present our estimate of the current status of the latest lattice results in the isospin symmetric limit. Based largely on references [21–25], which its authors considered to have the most reliable estimates of the systematic uncertainties, the FLAG Review [16] quoted as its summary of results obtained with $N_f = 2 + 1$ flavors of sea quarks:

$$\overline{m}_s = (93.8 \pm 1.5 \pm 1.9) \text{ MeV}, \quad (66.3)$$

$$\overline{m}_{ud} = (3.42 \pm 0.06 \pm 0.07) \text{ MeV} \quad (66.4)$$

and

$$\frac{\overline{m}_s}{\overline{m}_{ud}} = 27.46 \pm 0.15 \pm 0.41. \quad (66.5)$$

The masses are given in the $\overline{\text{MS}}$ scheme at a renormalization scale of 2 GeV. The first error comes from averaging the lattice results and the second is an estimate of the neglect of sea-quark effects from the charm and more massive quarks. Because of the systematic errors, these results are not simply the combinations of all the results in quadrature, but include a judgement of the remaining uncertainties. Since the different collaborations use different formulations of lattice QCD, the (relatively small) variations of the results between the groups provides important information about the reliability of the estimates.

Since the publication of the FLAG review [16] there have been a number of studies with $N_f = 2 + 1 + 1$ [26–28] and $N_f = 2 + 1$ [29] and a reasonable summary of the current status may be $\overline{m}_{ud} = (3.4 \pm 0.1) \text{ MeV}$, $\overline{m}_s = (93.5 \pm 2) \text{ MeV}$ and $\overline{m}_s/\overline{m}_{ud} = 27.5 \pm 0.3$.

To obtain the individual values of \overline{m}_u and \overline{m}_d requires the introduction of isospin breaking effects, including electromagnetism. In principle this can be done completely using lattice field theory. Such calculations are indeed beginning (note the recent computation of the neutron-proton mass splitting [30]) but are still at a relatively early stage. In practice therefore, \overline{m}_u and \overline{m}_d are extracted by combining lattice results with some elements of continuum phenomenology, most frequently based on chiral perturbation theory. Such studies include references [32,17,24,28,33,34] as well the Flavianet Lattice Averaging Group [43]. Based on these results we summarise the current status as

$$\frac{\overline{m}_u}{\overline{m}_d} = 0.46(5), \quad \overline{m}_u = 2.15(15) \text{ MeV}, \quad \overline{m}_d = 4.70(20) \text{ MeV}. \quad (66.6)$$

Again the masses are given in the $\overline{\text{MS}}$ scheme at a renormalization scale of 2 GeV. Of particular importance is the fact that $m_u \neq 0$ since there would have been no strong CP problem had m_u been equal to zero.

The quark mass ranges for the light quarks given in the listings combine the lattice and continuum values and use the PDG method for determining errors given in the introductory notes.

66.4.2. Chiral Perturbation Theory : For light quarks, one can use the techniques of chiral perturbation theory [6–8] to extract quark mass ratios. The mass term for light quarks in the QCD Lagrangian is

$$\overline{\Psi} M \Psi = \overline{\Psi}_L M \Psi_R + \overline{\Psi}_R M^\dagger \Psi_L, \quad (66.7)$$

where M is the light quark mass matrix,

$$M = \begin{pmatrix} m_u & 0 & 0 \\ 0 & m_d & 0 \\ 0 & 0 & m_s \end{pmatrix}, \quad (66.8)$$

$\Psi = (u, d, s)$, and L and R are the left- and right-chiral components of Ψ given by $\Psi_{L,R} = P_{L,R} \Psi$, $P_L = (1 - \gamma_5)/2$, $P_R = (1 + \gamma_5)/2$. The mass term is the only term in the QCD Lagrangian that mixes left- and right-handed quarks. In the limit $M \rightarrow 0$, there is an independent $SU(3) \times U(1)$ flavor symmetry for the left- and right-handed quarks. The vector $U(1)$ symmetry is baryon number; the axial $U(1)$ symmetry of the classical theory is broken in the quantum theory due to the anomaly. The remaining $G_\chi = SU(3)_L \times SU(3)_R$ chiral symmetry of the QCD Lagrangian is spontaneously broken to $SU(3)_V$, which, in the limit $M \rightarrow 0$, leads to eight massless Goldstone bosons, the π 's, K 's, and η .

The symmetry G_χ is only an approximate symmetry, since it is explicitly broken by the quark mass matrix M . The Goldstone bosons acquire masses which can be computed in a systematic expansion in M , in terms of low-energy constants, which are unknown nonperturbative parameters of the effective theory, and are not fixed by the symmetries. One treats the quark mass matrix M as an external field that transforms under G_χ

6 66. Quark masses

as $M \rightarrow LMR^\dagger$, where $\Psi_L \rightarrow L\Psi_L$ and $\Psi_R \rightarrow R\Psi_R$ are the $SU(3)_L$ and $SU(3)_R$ transformations, and writes down the most general Lagrangian invariant under G_χ . Then one sets M to its given constant value Eq. (66.8), which implements the symmetry breaking. To first order in M one finds that [9]

$$\begin{aligned}
m_{\pi^0}^2 &= B(m_u + m_d) , \\
m_{\pi^\pm}^2 &= B(m_u + m_d) + \Delta_{\text{em}} , \\
m_{K^0}^2 &= m_{\bar{K}^0}^2 = B(m_d + m_s) , \\
m_{K^\pm}^2 &= B(m_u + m_s) + \Delta_{\text{em}} , \\
m_\eta^2 &= \frac{1}{3}B(m_u + m_d + 4m_s) ,
\end{aligned} \tag{66.9}$$

with two unknown constants B and Δ_{em} , the electromagnetic mass difference. From Eq. (66.9), one can determine the quark mass ratios [9]

$$\begin{aligned}
\frac{m_u}{m_d} &= \frac{2m_{\pi^0}^2 - m_{\pi^+}^2 + m_{K^+}^2 - m_{K^0}^2}{m_{K^0}^2 - m_{K^+}^2 + m_{\pi^+}^2} = 0.56 , \\
\frac{m_s}{m_d} &= \frac{m_{K^0}^2 + m_{K^+}^2 - m_{\pi^+}^2}{m_{K^0}^2 + m_{\pi^+}^2 - m_{K^+}^2} = 20.2 ,
\end{aligned} \tag{66.10}$$

to lowest order in chiral perturbation theory, with an error which will be estimated below. Since the mass ratios extracted using chiral perturbation theory use the symmetry transformation property of M under the chiral symmetry G_χ , it is important to use a renormalization scheme for QCD that does not change this transformation law. Any mass independent subtraction scheme such as $\overline{\text{MS}}$ is suitable. The ratios of quark masses are scale independent in such a scheme, and Eq. (66.10) can be taken to be the ratio of $\overline{\text{MS}}$ masses. Chiral perturbation theory cannot determine the overall scale of the quark masses, since it uses only the symmetry properties of M , and any multiple of M has the same G_χ transformation law as M .

Chiral perturbation theory is a systematic expansion in powers of the light quark masses. The typical expansion parameter is $m_K^2/\Lambda_\chi^2 \sim 0.25$ if one uses $SU(3)$ chiral symmetry, and $m_\pi^2/\Lambda_\chi^2 \sim 0.02$ if instead one uses $SU(2)$ chiral symmetry. Electromagnetic effects at the few percent level also break $SU(2)$ and $SU(3)$ symmetry. The mass formulæ Eq. (66.9) were derived using $SU(3)$ chiral symmetry, and are expected to have approximately a 25% uncertainty due to second order corrections. This estimate of the uncertainty is consistent with the lattice results found in Eq. (66.3)-Eq. (66.5) and more recent calculations.

There is a subtlety which arises when one tries to determine quark mass ratios at second order in chiral perturbation theory. The second order quark mass term [10]

$$\left(M^\dagger\right)^{-1} \det M^\dagger \tag{66.11}$$

(which can be generated by instantons) transforms in the same way under G_χ as M . Chiral perturbation theory cannot distinguish between M and $(M^\dagger)^{-1} \det M^\dagger$; one can make the replacement $M \rightarrow M(\lambda) = M + \lambda M (M^\dagger M)^{-1} \det M^\dagger$ in the chiral Lagrangian,

$$\begin{aligned} M(\lambda) &= \text{diag}(m_u(\lambda), m_d(\lambda), m_s(\lambda)) \\ &= \text{diag}(m_u + \lambda m_d m_s, m_d + \lambda m_u m_s, m_s + \lambda m_u m_d), \end{aligned} \quad (66.12)$$

and leave all observables unchanged.

The combination

$$\left(\frac{m_u}{m_d}\right)^2 + \frac{1}{Q^2} \left(\frac{m_s}{m_d}\right)^2 = 1 \quad (66.13)$$

where

$$Q^2 = \frac{m_s^2 - \hat{m}^2}{m_d^2 - m_u^2}, \quad \hat{m} = \frac{1}{2}(m_u + m_d),$$

is insensitive to the transformation in Eq. (66.12). Eq. (66.13) gives an ellipse in the $m_u/m_d - m_s/m_d$ plane. The ellipse is well-determined by chiral perturbation theory, but the exact location on the ellipse, and the absolute normalization of the quark masses, has larger uncertainties. Q is determined to be in the range 21–25 from $\eta \rightarrow 3\pi$ decay and the electromagnetic contribution to the $K^{+-} - K^0$ and $\pi^{+-} - \pi^0$ mass differences [11].

The absolute normalization of the quark masses cannot be determined using chiral perturbation theory. Other methods, such as lattice simulations discussed above or spectral function sum rules [12,13] for hadronic correlation functions, which we review next are necessary.

66.4.3. Sum Rules : Sum rule methods have been used extensively to determine quark masses and for illustration we briefly discuss here their application to hadronic τ decays [14]. Other applications involve very similar techniques.

The experimentally measured quantity is R_τ ,

$$\frac{dR_\tau}{ds} = \frac{d\Gamma/ds(\tau^- \rightarrow \text{hadrons} + \nu_\tau(\gamma))}{\Gamma(\tau^- \rightarrow e^- \bar{\nu}_e \nu_\tau(\gamma))} \quad (66.14)$$

the hadronic invariant mass spectrum in semihadronic τ decay, normalized to the leptonic τ decay rate. It is useful to define q as the total momentum of the hadronic final state, so $s = q^2$ is the hadronic invariant mass. The total hadronic τ decay rate R_τ is then given by integrating dR_τ/ds over the kinematically allowed range $0 \leq s \leq M_\tau^2$.

R_τ can be written as

$$\begin{aligned} R_\tau &= 12\pi \int_0^{M_\tau^2} \frac{ds}{M_\tau^2} \left(1 - \frac{s}{M_\tau^2}\right)^2 \\ &\quad \times \left[\left(1 + 2\frac{s}{M_\tau^2}\right) \text{Im} \Pi^T(s) + \text{Im} \Pi^L(s) \right] \end{aligned} \quad (66.15)$$

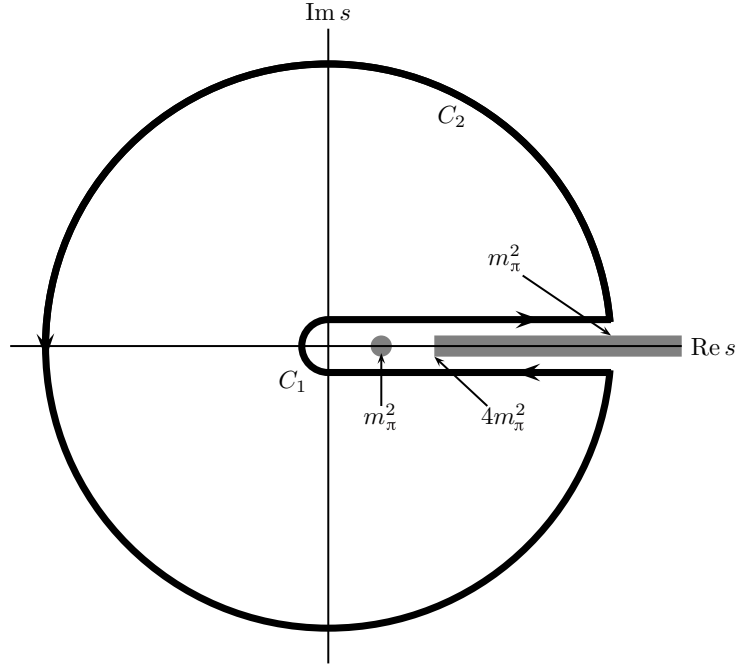


Figure 66.1: The analytic structure of $\Pi(s)$ in the complex s -plane. The contours C_1 and C_2 are the integration contours discussed in the text.

where $s = q^2$, and the hadronic spectral functions $\Pi^{L,T}$ are defined from the time-ordered correlation function of two weak currents is the time-ordered correlator of the weak interaction current ($j^\mu(x)$ and $j^\nu(0)$) by

$$\Pi^{\mu\nu}(q) = i \int d^4x e^{iq \cdot x} \langle 0 | T (j^\mu(x) j^\nu(0)^\dagger) | 0 \rangle, \quad (66.16)$$

$$\Pi^{\mu\nu}(q) = (-g^{\mu\nu} + q^\mu q^\nu) \Pi^T(s) + q^\mu q^\nu \Pi^L(s), \quad (66.17)$$

and the decomposition Eq. (66.17) is the most general possible structure consistent with Lorentz invariance.

By the optical theorem, the imaginary part of $\Pi^{\mu\nu}$ is proportional to the total cross-section for the current to produce all possible states. A detailed analysis including the phase space factors leads to Eq. (66.15). The spectral functions $\Pi^{L,T}(s)$ are analytic in the complex s plane, with singularities along the real axis. There is an isolated pole at $s = m_\pi^2$, and single- and multi-particle singularities for $s \geq 4m_\pi^2$, the two-particle threshold. The discontinuity along the real axis is $\Pi^{L,T}(s + i0^+) - \Pi^{L,T}(s - i0^+) = 2i \text{Im} \Pi^{L,T}(s)$. As a result, Eq. (66.15) can be rewritten with the replacement $\text{Im} \Pi^{L,T}(s) \rightarrow -i\Pi^{L,T}(s)/2$, and the integration being over the contour C_1 . Finally, the contour C_1 can be deformed to C_2 without crossing any singularities, and so leaving the integral unchanged. One

can derive a series of sum rules analogous to Eq. (66.15) by weighting the differential τ hadronic decay rate by different powers of the hadronic invariant mass,

$$R_\tau^{kl} = \int_0^{M_\tau^2} ds \left(1 - \frac{s}{M_\tau^2}\right)^k \left(\frac{s}{M_\tau^2}\right)^l \frac{dR_\tau}{ds} \quad (66.18)$$

where dR_τ/ds is the hadronic invariant mass distribution in τ decay normalized to the leptonic decay rate. This leads to the final form of the sum rule(s),

$$R_\tau^{kl} = -6\pi i \int_{C_2} \frac{ds}{M_\tau^2} \left(1 - \frac{s}{M_\tau^2}\right)^{2+k} \left(\frac{s}{M_\tau^2}\right)^l \times \left[\left(1 + 2\frac{s}{M_\tau^2}\right) \Pi^T(s) + \Pi^L(s) \right]. \quad (66.19)$$

The manipulations so far are completely rigorous and exact, relying only on the general analytic structure of quantum field theory. The left-hand side of the sum rule Eq. (66.19) is obtained from experiment. The right hand-side can be computed for s far away from any physical cuts using the operator product expansion (OPE) for the time-ordered product of currents in Eq. (66.16), and QCD perturbation theory. The OPE is an expansion for the time-ordered product Eq. (66.16) in a series of local operators, and is an expansion about the $q \rightarrow \infty$ limit. It gives $\Pi(s)$ as an expansion in powers of $\alpha_s(s)$ and Λ_{QCD}^2/s , and is valid when s is far (in units of Λ_{QCD}^2) from any singularities in the complex s -plane.

The OPE gives $\Pi(s)$ as a series in α_s , quark masses, and various non-perturbative vacuum matrix element. By computing $\Pi(s)$ theoretically, and comparing with the experimental values of R_τ^{kl} , one determines various parameters such as α_s and the quark masses. The theoretical uncertainties in using Eq. (66.19) arise from neglected higher order corrections (both perturbative and non-perturbative), and because the OPE is no longer valid near the real axis, where Π has singularities. The contribution of neglected higher order corrections can be estimated as for any other perturbative computation. The error due to the failure of the OPE is more difficult to estimate. In Eq. (66.19), the OPE fails on the endpoints of C_2 that touch the real axis at $s = M_\tau^2$. The weight factor $(1 - s/M_\tau^2)$ in Eq. (66.19) vanishes at this point, so the importance of the endpoint can be reduced by choosing larger values of k .

66.5. Heavy quarks

For heavy-quark physics one can exploit the fact that $m_Q \gg \Lambda_{\text{QCD}}$ to construct effective theories (m_Q is the mass of the heavy quark Q). The masses and decay rates of hadrons containing a single heavy quark, such as the B and D mesons can be determined using the heavy quark effective theory (HQET) [45]. The theoretical calculations involve radiative corrections computed in perturbation theory with an expansion in $\alpha_s(m_Q)$ and non-perturbative corrections with an expansion in powers of Λ_{QCD}/m_Q . Due to the asymptotic nature of the QCD perturbation series, the two kinds of corrections are

10 66. Quark masses

intimately related; an example of this are renormalon effects in the perturbative expansion which are associated with non-perturbative corrections.

Systems containing two heavy quarks such as the Υ or J/Ψ are treated using non-relativistic QCD (NRQCD) [46]. The typical momentum and energy transfers in these systems are $\alpha_s m_Q$, and $\alpha_s^2 m_Q$, respectively, so these bound states are sensitive to scales much smaller than m_Q . However, smeared observables, such as the cross-section for $e^+e^- \rightarrow \bar{b}b$ averaged over some range of s that includes several bound state energy levels, are better behaved and only sensitive to scales near m_Q . For this reason, most determinations of the c, b quark masses using perturbative calculations compare smeared observables with experiment [47–49].

There are many continuum extractions of the c and b quark masses, some with quoted errors of 10 MeV or smaller. There are systematic effects of comparable size, which are typically not included in these error estimates. Reference [41], for example, shows that even though the error estimate of m_c using the rapid convergence of the α_s perturbation series is only a few MeV, the central value of m_c can differ by a much larger amount depending on which algorithm (all of which are formally equally good) is used to determine m_c from the data. This leads to a systematic error from perturbation theory of around 20 MeV for the c quark and 25 MeV for the b quark. Electromagnetic effects, which also are important at this precision, are often not included. For this reason, we inflate the errors on the continuum extractions of m_c and m_b . The average values of m_c and m_b from continuum determinations are (see Sec. G for the 1S scheme)

$$\begin{aligned}\bar{m}_c(\bar{m}_c) &= (1.28 \pm 0.025) \text{ GeV} \\ \bar{m}_b(\bar{m}_b) &= (4.18 \pm 0.03) \text{ GeV}, \quad m_b^{1S} = (4.65 \pm 0.03) \text{ GeV}.\end{aligned}$$

Lattice simulations of QCD lead to discretization errors which are powers of $m_Q a$ (modulated by logarithms); the power depends on the formulation of lattice QCD being used and in most cases is quadratic. Clearly these errors can be reduced by performing simulations at smaller lattice spacings, but also by using *improved* discretizations of the theory. Recently, with more powerful computing resources, better algorithms and techniques, it has become possible to perform simulations in the charm quark region and beyond, also decreasing the extrapolation which has to be performed to reach the b -quark. A novel approach proposed in [64] has been to compare the lattice results for moments of correlation functions of $c\bar{c}$ quark-bilinear operators to perturbative calculations of the same quantities at 4-loop order. In this way both the strong coupling constant and the charm quark mass can be determined with remarkably small errors; in particular $\bar{m}_c(\bar{m}_c) = 1.273(6) \text{ GeV}$ [36]. This lattice determination also uses the perturbative expression for the current-current correlator, and so has the perturbation theory systematic error discussed above. Recent updates using this correlator method, both with a very similar result, can be found in [27,37]. It should be remembered that these results were obtained in QCD with exact isospin symmetry; isospin breaking effects, including electromagnetism may well be larger or of the order of the quoted uncertainty.

As the range of heavy-quark masses which can be used in numerical simulations increases, results obtained by extrapolating the results to b -physics are becoming ever

more reliable (see e.g. [27]) . Traditionally however, the main approach to controlling the discretization errors in lattice studies of heavy quark physics has been to perform simulations of the effective theories such as HQET and NRQCD. This remains an important technique, both in its own right and in providing additional information for extrapolations from lower masses to the bottom region. Using effective theories, m_b is obtained from what is essentially a computation of the difference of $M_{H_b} - m_b$, where M_{H_b} is the mass of a hadron H_b containing a b -quark. The relative error on m_b is therefore much smaller than that for $M_{H_b} - m_b$. The principal systematic errors are the matching of the effective theories to QCD and the presence of power divergences in a^{-1} in the $1/m_b$ corrections which have to be subtracted numerically. The use of HQET or NRQCD is less precise for the charm quark, but in this case, as mentioned above, direct QCD simulations are now possible.

66.6. Pole Mass

For an observable particle such as the electron, the position of the pole in the propagator is the definition of its mass. In QCD this definition of the quark mass is known as the pole mass. It is known that the on-shell quark propagator has no infrared divergences in perturbation theory [52,53], so this provides a perturbative definition of the quark mass. The pole mass cannot be used to arbitrarily high accuracy because of nonperturbative infrared effects in QCD. The full quark propagator has no pole because the quarks are confined, so that the pole mass cannot be defined outside of perturbation theory. The relation between the pole mass m_Q and the $\overline{\text{MS}}$ mass \overline{m}_Q is known to three loops [54,55,56,57]

$$\begin{aligned}
 m_Q = \overline{m}_Q(\overline{m}_Q) & \left\{ 1 + \frac{4\overline{\alpha}_s(\overline{m}_Q)}{3\pi} \right. \\
 & + \left[-1.0414 \sum_k \left(1 - \frac{4}{3} \frac{\overline{m}_{Q_k}}{\overline{m}_Q} \right) + 13.4434 \right] \left[\frac{\overline{\alpha}_s(\overline{m}_Q)}{\pi} \right]^2 \\
 & \left. + \left[0.6527N_L^2 - 26.655N_L + 190.595 \right] \left[\frac{\overline{\alpha}_s(\overline{m}_Q)}{\pi} \right]^3 \right\}, \tag{66.20}
 \end{aligned}$$

where $\overline{\alpha}_s(\mu)$ is the strong interaction coupling constants in the $\overline{\text{MS}}$ scheme, and the sum over k extends over the N_L flavors Q_k lighter than Q . The complete mass dependence of the α_s^2 term can be found in [54]; the mass dependence of the α_s^3 term is not known. For the b -quark, Eq. (66.20) reads

$$m_b = \overline{m}_b(\overline{m}_b) [1 + 0.10 + 0.05 + 0.03], \tag{66.21}$$

where the contributions from the different orders in α_s are shown explicitly. The two and three loop corrections are comparable in size and have the same sign as the one loop term. This is a signal of the asymptotic nature of the perturbation series [there is

12 66. Quark masses

a renormalon in the pole mass]. Such a badly behaved perturbation expansion can be avoided by directly extracting the $\overline{\text{MS}}$ mass from data without extracting the pole mass as an intermediate step.

66.7. Numerical values and caveats

The quark masses in the particle data listings have been obtained by using a wide variety of methods. Each method involves its own set of approximations and uncertainties. In most cases, the errors are an estimate of the size of neglected higher-order corrections or other uncertainties. The expansion parameters for some of the approximations are not very small (for example, they are $m_K^2/\Lambda_\chi^2 \sim 0.25$ for the chiral expansion and $\Lambda_{\text{QCD}}/m_b \sim 0.1$ for the heavy-quark expansion), so an unexpectedly large coefficient in a neglected higher-order term could significantly alter the results. It is also important to note that the quark mass values can be significantly different in the different schemes.

The heavy quark masses obtained using HQET, QCD sum rules, or lattice gauge theory are consistent with each other if they are all converted into the same scheme and scale. We have specified all masses in the $\overline{\text{MS}}$ scheme. For light quarks, the renormalization scale has been chosen to be $\mu = 2 \text{ GeV}$. The light quark masses at 1 GeV are significantly different from those at 2 GeV, $\overline{m}(1 \text{ GeV})/\overline{m}(2 \text{ GeV}) \sim 1.33$. It is conventional to choose the renormalization scale equal to the quark mass for a heavy quark, so we have quoted $\overline{m}_Q(\mu)$ at $\mu = \overline{m}_Q$ for the c and b quarks. Recent analyses of inclusive B meson decays have shown that recently proposed mass definitions lead to a better behaved perturbation series than for the $\overline{\text{MS}}$ mass, and hence to more accurate mass values. We have chosen to also give values for one of these, the b quark mass in the 1S-scheme [58,59]. Other schemes that have been proposed are the PS-scheme [60] and the kinetic scheme [61].

If necessary, we have converted values in the original papers to our chosen scheme using two-loop formulæ. It is important to realize that our conversions introduce significant additional errors. In converting to the $\overline{\text{MS}}$ b -quark mass, for example, the three-loop conversions from the 1S and pole masses give values about 35 MeV and 135 MeV lower than the two-loop conversions. The uncertainty in $\alpha_s(M_Z) = 0.1181(13)$ gives an uncertainty of $\pm 10 \text{ MeV}$ and $\pm 35 \text{ MeV}$ respectively in the same conversions. We have not added these additional errors when we do our conversions. The α_s value in the conversion is correlated with the α_s value used in determining the quark mass, so the conversion error is not a simple additional error on the quark mass.

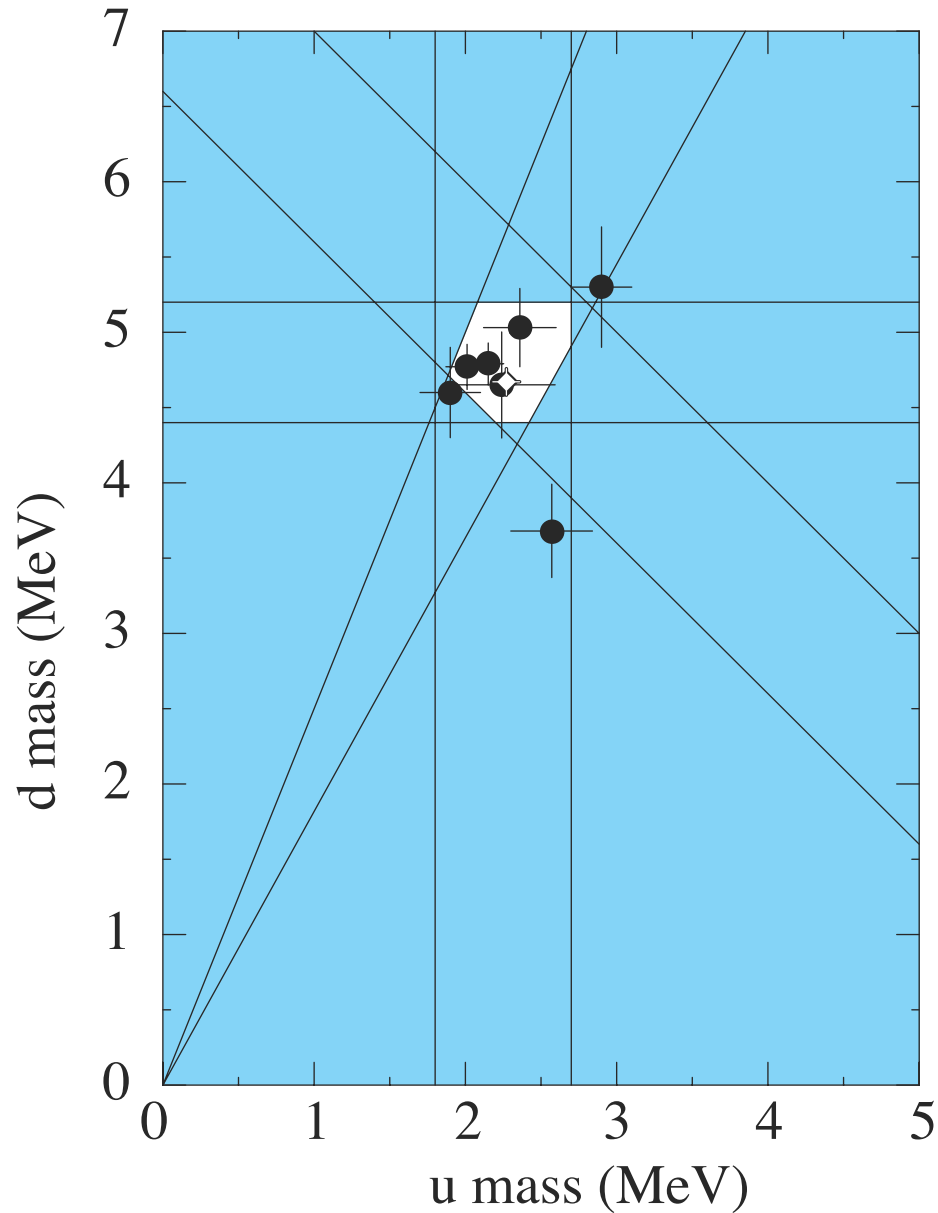


Figure 66.2: The allowed region (shown in white) for up quark and down quark masses. This region was determined in part from papers reporting values for m_u and m_d (data points shown) and in part from analysis of the allowed ranges of other mass parameters (see Fig. 66.3). The parameter $(m_u + m_d)/2$ yields the two downward-sloping lines, while m_u/m_d yields the two rising lines originating at $(0,0)$. There are two overlapping data points, so one of them is shown as a white diamond (it has very small error bars).

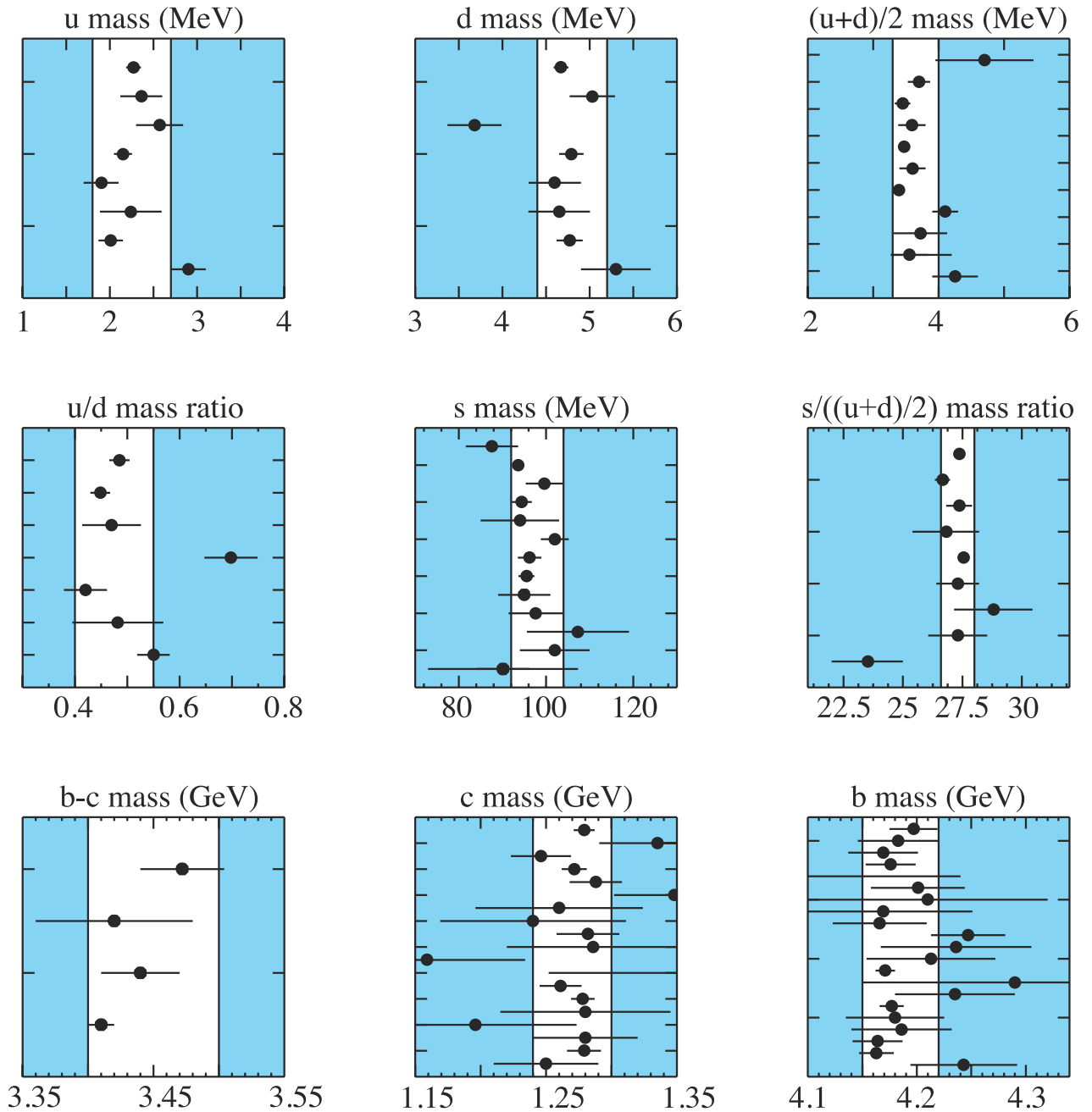


Figure 66.3: The values of each quark mass parameter taken from the Data Listings. The points are in chronological order with the more recent measurements at the top. Points from papers reporting no error bars are colored grey. The shaded regions indicate values excluded by our evaluations; some regions were determined in part through examination of Fig. 66.2.

References:

1. See the review of QCD in this volume..
2. A.V. Manohar and H. Georgi, Nucl. Phys. **B234**, 189 (1984).
3. K.G. Chetyrkin, Phys. Lett. **B404**, 161 (1997).
4. J.A.M. Vermaseren, S.A. Larin, and T. van Ritbergen, Phys. Lett. **B405**, 327 (1997).
5. K.G. Chetyrkin, B.A. Kniehl, and M. Steinhauser, Nucl. Phys. **B510**, 61 (1998).
6. S. Weinberg, Physica **96A**, 327 (1979).
7. J. Gasser and H. Leutwyler, Ann. Phys. **158**, 142 (1984).
8. For a review, see A. Pich, Rept. on Prog. in Phys. **58**, 563 (1995).
9. S. Weinberg, Trans. N.Y. Acad. Sci. **38**, 185 (1977).
10. D.B. Kaplan and A.V. Manohar, Phys. Rev. Lett. **56**, 2004 (1986).
11. H. Leutwyler, Phys. Lett. **B374**, 163 (1996).
12. S. Weinberg, Phys. Rev. Lett. **18**, 507 (1967).
13. M.A. Shifman, A.I. Vainshtein, and V.I. Zakharov, Nucl. Phys. **B147**, 385 (1979).
14. E. Braaten, S. Narison, and A. Pich, Nucl. Phys. **B373**, 581 (1992).
15. C. Bernard *et al.*, PoS **LAT2007** (2007) 090.
16. S. Aoki *et al.* [FLAG Collab.], Eur. Phys. J. **C74**, 2890 (2014).
17. A. Bazavov *et al.*, arXiv:0903.3598 [hep-lat].
18. C. Aubin *et al.* [HPQCD Collab.], Phys. Rev. **D70**, 031504 (2004).
19. C. Aubin *et al.* [MILC Collab.], Phys. Rev. **D70**, 114501 (2004).
20. B. Blossier *et al.* [ETM Collab.], Phys. Rev. **D82**, 114513 (2010).
21. A. Bazavov *et al.* [MILC Collab.], PoS **CD09** (2009) 007.
22. A. Bazavov *et al.*, PoS **LATTICE2010** (2010) 083.
23. S. Durr *et al.*, Phys. Lett. **B701**, 265 (2011).
24. S. Durr *et al.*, JHEP **1108**, 148 (2011).
25. R. Arthur *et al.* [RBC and UKQCD Collabs.], Phys. Rev. **D87**, 094514 (2013).
26. A. Bazavov *et al.* [Fermilab Lattice and MILC Collabs.], Phys. Rev. **D90**, 074509 (2014).
27. B. Chakraborty *et al.*, Phys. Rev. **D91**, 054508 (2015).
28. N. Carrasco *et al.* [European Twisted Mass Collab.], Nucl. Phys. **B887**, 19 (2014).
29. “Domain wall QCD with physical quark masses,” T. Blum *et al.* [RBC and UKQCD Collabs.], arXiv:1411.7017 [hep-lat].
30. S. Borsanyi *et al.*, Science **347**, 1452 (2015).
31. Y. Aoki *et al.* [RBC and UKQCD Collabs.], Phys. Rev. **D83**, 074508 (2011).
32. S. Basak *et al.* [MILC Collab.], J. Phys. Conf. Ser. **640** (2015) 1, 012052.
33. T. Blum *et al.*, Phys. Rev. **D82**, 094508 (2010).
34. S. Aoki *et al.*, Phys. Rev. **D86**, 034507 (2012).
35. C.T.H. Davies *et al.*, Phys. Rev. Lett. **104**, 132003 (2010).
36. C. McNeile *et al.*, Phys. Rev. **D82**, 034512 (2010).
37. K. Nakayama, B. Fahy, and S. Hashimoto, arXiv:1511.09163 [hep-lat]..
38. C. Aubin *et al.* [MILC Collab.], Nucl. Phys. (Proc. Supp.) **140**, 231 (2005).
39. C. Aubin *et al.* [MILC Collab.], Phys. Rev. **D70**, 114501 (2004).
40. G. Colangelo *et al.*, Eur. Phys. J. **C71**, 1695 (2011).

16 *66. Quark masses*

41. B. Dehnadi *et al.*, [arXiv:1102.2264](#) [hep-ph].
42. T. Blum *et al.*, Phys. Rev. **D76**, 114508 (2007).
43. G. Colangelo *et al.*, Eur. Phys. J. **C71**, 1695 (2011).
44. A. Ali Khan *et al.* [CP-PACS Collab.], Phys. Rev. **D65**, 054505 (2002); [Erratum-
ibid. D **67** (2003) 059901].
45. N. Isgur and M.B. Wise, Phys. Lett. **B232**, 113 (1989), *ibid.* **B237**, 527 (1990).
46. G.T. Bodwin, E. Braaten, and G.P. Lepage, Phys. Rev. **D51**, 1125 (1995).
47. A.H. Hoang, Phys. Rev. **D61**, 034005 (2000).
48. K. Melnikov and A. Yelkhovsky, Phys. Rev. **D59**, 114009 (1999).
49. M. Beneke and A. Signer, Phys. Lett. **B471**, 233 (1999).
50. A.X. El-Khadra, A.S. Kronfeld, and P.B. Mackenzie, Phys. Rev. **D55**, 3933 (1997).
51. S. Aoki, Y. Kuramashi, and S.i. Tominaga, Prog. Theor. Phys. **109**, 383 (2003).
52. R. Tarrach, Nucl. Phys. **B183**, 384 (1981).
53. A. Kronfeld, Phys. Rev. **D58**, 051501 (1998).
54. N. Gray *et al.*, Z. Phys. **C48**, 673 (1990).
55. D.J. Broadhurst, N. Gray, and K. Schilcher, Z. Phys. **C52**, 111 (1991).
56. K.G. Chetyrkin and M. Steinhauser, Phys. Rev. Lett. **83**, 4001 (1999).
57. K. Melnikov and T. van Ritbergen, Phys. Lett. **B482**, 99 (2000).
58. A.H. Hoang, Z. Ligeti, A.V. Manohar, Phys. Rev. Lett. **82**, 277 (1999).
59. A.H. Hoang, Z. Ligeti, A.V. Manohar, Phys. Rev. **D59**, 074017 (1999).
60. M. Beneke, Phys. Lett. **B434**, 115 (1998).
61. P. Gambino and N. Uraltsev, Eur. Phys. J. **C34**, 181 (2004).
62. G. Martinelli *et al.*, Nucl. Phys. **B445**, 81 (1995).
63. K. Jansen *et al.*, Phys. Lett. **B372**, 275 (1996).
64. I. Allison *et al.* [HPQCD Collab.], Phys. Rev. **D78**, 054513 (2008).